

## Absolute Measurement of Two-Photon Cross Sections

J. P. Hermann and J. Ducuing

*Laboratoire d'Optique Quantique du Centre National de la Recherche Scientifique, 91 Orsay, France  
and Université Paris-Sud, 91 Orsay, France*

(Received 28 December 1971)

A method is presented which yields two-photon cross-section values  $\delta$  which are independent of the statistical properties of the light beam. A two-cell arrangement is used in which the fluorescence intensity produced by two-photon absorption of a laser beam is compared to that due to one-photon absorption of the harmonic light generated by the same beam in a quartz slab at the top of a Maker fringe. The measurement does not require a calibration of the detecting channels but relies on the knowledge of the one-photon cross section at the harmonic frequency and of the appropriate component of the nonlinear susceptibility tensor  $\chi^{(2)}$ . Values of  $\delta$  ( $\lambda = 6943 \text{ \AA}$ ) are presented for several organic molecules and compared to those obtained by other methods.

### I. INTRODUCTION

Since the first observation of two-photon absorption by Kaiser and Garrett,<sup>1</sup> a large amount of work has been done, both on the study of the absorption process and its use for spectroscopic purposes. To this last aim, refined experimental methods have been devised and detailed two-photon spectra of molecules and crystals can now be obtained.<sup>2</sup> A considerably smaller effort has been devoted to accurate quantitative studies of the transition strengths. The quantity of interest here is the two-photon cross-section coefficient  $\delta$ , which relates the transition probability per unit time  $dp/dt$  to the square of the photon flux density  $F$

$$\frac{dp}{dt} = \delta F^2. \quad (1)$$

There is substantial disagreement between the published values of this quantity, as shown by the large scatter of the results obtained by various authors for the anthracene molecule in solution (see Table II). This state of affairs is unfortunate, as accurate and reliable values of two-photon cross sections are needed, not only for the interpretation of spectra, particularly in the case of symmetry-forbidden vibrationally induced transitions, but also for the study of two-photon emission processes.<sup>3</sup>

There exists a large variety of methods of measurement. We shall limit our considerations to those which are most widely used and easily interpreted. In the most direct one the absorption of a light beam with half the transition frequency  $\omega_{ba}$  is studied as a function of intensity.<sup>4,5</sup> Equivalently, one can measure the absorption induced on a weak probing beam with frequency  $\omega_1$  by an intense beam at  $\omega_{ba} - \omega_1$ .<sup>6,7</sup> Both these methods yield results which depend strongly on the spatial and temporal coherence of the light beams.<sup>2</sup> Furthermore they are of limited sensitivity, as to secure measurable

absorption coefficients with reasonable light intensities for which spurious effects are avoided, both the cross section and the molecule concentration must be high. In another family of experiments, a fluorescent emission following the two-quantum absorption is detected.<sup>1,8</sup> A typical arrangement is shown on Fig. 1. The sample under study is irradiated by a laser beam; part of the fluorescence is collected by an optical system (O), and after appropriate filtering, by system (F) (interference filters or monochromator), is detected by a photomultiplier. If the laser flux distribution and the fluorescence quantum yield are known, the two-photon cross section can be deduced from the measurement of the fluorescence intensity.

There are two main difficulties associated with this procedure. A first one is to make an accurate measurement of the fluorescence. Indeed, this requires a precise knowledge of the following factors: (i) the fraction of the emitted light, which is collected; (ii) the transmission of the collecting and filtering systems; (iii) the photomultiplier gain; and (iv) the photocathode quantum efficiency, all of which are sources of possibly large errors.

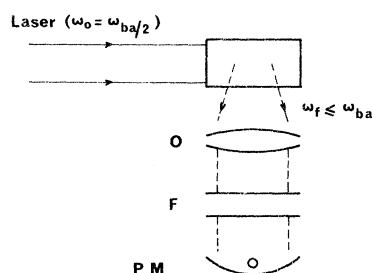


FIG. 1. Basic setup of a two-photon experiment using the fluorescence light emitted by a sample; O is the optical device (collecting lenses), F are the filters, and PM is the light detector.

To obviate the need for the corresponding measurements, Galanin and Chizhikova<sup>9</sup> have calibrated the detecting channel by observing the fluorescence consecutive to one-photon absorption of incoherent light with a frequency approximately twice that of the laser. If the same final state is reached in both transitions, the ratio of the number of excited molecules is obtained directly from a comparison of the photomultiplier currents, without any need for the knowledge of the previous factors or of the quantum yield. The second difficulty arises when one attempts to deduce the cross sections from the relative transition probabilities. Call  $F_1(\vec{r}, t)$  and  $F_2(\vec{r}, t)$  the laser and calibrating light photon fluxes per unit area, respectively. The photocurrents detected, respectively, after one- and two-photon excitation are

$$I_{1P}(t) = CN_0\sigma D_t \int_V F_2(\vec{r}, t) d\vec{r} \quad , \quad (2)$$

$$I_{2P}(t) = CN_0\delta D_t \int_V F_1^2(\vec{r}, t) d\vec{r} \quad , \quad (3)$$

where  $C$  is a calibrating constant, which includes the previous four factors and the fluorescence quantum yield;  $V$  is the observed volume;  $N_0$  the number of molecules per unit volume;  $\sigma$  and  $\delta$  the one- and two-photon cross sections; and  $D_t$  is a time operator which expresses the response of the detecting channel and includes the finite lifetime of the upper state of the fluorescent transition as well as the time constant of the photomultiplier and associated circuitry. In the simple case where this response can be characterized by a time constant  $T$ , then

$$D_t = \frac{1}{T} \int_0^t dt' e^{-(t-t')/T} \quad .$$

As shown by Eqs. (2) and (3), the calibration achieved by this method depends in general on the spatial and temporal coherence of the fields. Aleksandrov and Bredikhin<sup>10</sup> used for the calibrating light the harmonic radiation generated by a single transverse mode beam in a potassium dihydrogen phosphate (KDP) crystal under phase-matching conditions. They determined the spatial structure of the laser and harmonic beams by photographic measurements and their energy by calorimetric techniques. Unfortunately, it is well known that at phase matching the coherence properties of the harmonic beam are not simply deduced from those of the fundamental beam.<sup>11-13</sup> Thus  $F_2$  can have a behavior in time and space very different from that of  $F_1^2$ , and the measured value of  $\delta$  will be strongly dependent on the properties of the fundamental beam. Accurate single transverse and longitudinal mode operation of a Q-switched ruby laser is always difficult, particularly at the high

power level necessary for the very efficient doubling used by these authors. Time- and space-integrated measurements by photographic and calorimetric techniques cannot remove this uncertainty.

In this paper we demonstrate a simple method which eliminates any need for control or knowledge of the statistical properties of the laser beam and yields a value of  $\delta$  in terms of known physical quantities. After exposing the principles of this method we give a detailed description of the experimental procedure and discuss some results.

## II. PRINCIPLES

The method consists of comparing the fluorescence produced by direct two-photon laser excitation to that following the absorption of the harmonic radiation generated in a thin nonlinear platelet set at the maximum of the first Maker fringe.<sup>14,15</sup> It rests essentially on the observation that, if certain simple conditions are met, on the exit face of the platelet the harmonic flux density at point  $\vec{r}$  and time  $t$  is given by

$$F_2(\vec{r}, t) = QF_1^2(\vec{r}, t) \quad , \quad (4)$$

where  $F_1(\vec{r}, t)$  is the fundamental flux density and  $Q$ , a quantity independent of space and time, is a function<sup>15</sup> of the linear and nonlinear optical properties of the material. This relation is derived with its validity conditions in the Appendix. Figure 2 gives a very schematic diagram of the experimental arrangement. A laser beam ( $\omega_0$ ) propagates through a quartz platelet where it creates harmonic radiation ( $2\omega_0$ ). The two cells  $C_A$  and  $C_B$  contain the substance to be studied. Appropriate filters  $T_A$  and  $T_B$  select the irradiating frequencies: Cell  $B$  receives only the harmonic frequency, whereas cell  $A$  can be irradiated by either  $\omega_0$  or  $2\omega_0$ ; the transverse structure of the beams is the same, on the quartz plate,  $C_A$  and  $C_B$ . The emitted fluorescence is detected by photoelectric detectors  $D_A$  and  $D_B$  with identical time response. For a first laser pulse with flux density  $F_1(\vec{r}, t)$ ,  $T_A$  transmits only  $2\omega_0$  with a transmission coefficient  $t_A(2\omega_0)$ . The corresponding currents detected by  $D_A$  and  $D_B$  are

$$\begin{aligned} I_A &= t_A(2\omega_0)C_A\sigma D_t \int_S d^2r F_2(\vec{r}, t) \\ &= t_A(2\omega_0)C_A\sigma Q D_t \int_S d^2r F_1^2(\vec{r}, t) \quad , \end{aligned} \quad (5)$$

$$I_B = C_B\sigma Q D_t \int_S d^2r F_1^2(\vec{r}, t) \quad . \quad (6)$$

For a second laser pulse  $F'_1(\vec{r}, t)$ ,  $T_A$  transmits only  $\omega_0$ , then

$$I'_A = t_A^2(\omega_0)C_A\delta D_t \int_S d^2r F_1'^2(\vec{r}, t) \quad , \quad (7)$$

$$I'_B = C_B\sigma Q D_t \int_S d^2r F_1'^2(\vec{r}, t) \quad . \quad (8)$$

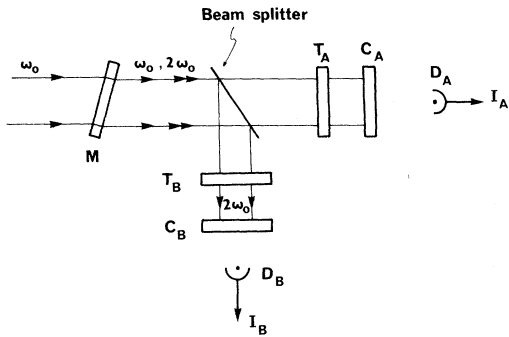


FIG. 2. Principle of the present method: A designates measurement; B designates reference,  $T_A$  is the  $\omega_0$  or  $2\omega_0$  transmitting filter,  $T_B$  is the  $2\omega_0$  transmitting filter,  $C_A$  and  $C_B$  are cells containing the fluorescent dye, and  $D_A$  and  $D_B$  are detectors.

In relations (5)–(8)  $C_A$  and  $C_B$  are calibrating coefficients,  $D_t$  is the time response operator (the same for both channels), and the transverse integration is performed over the cross section of the beams. From these relations, we obtain

$$\delta = \sigma Q (I_B I'_A / I_A I'_B) [t_A (2\omega_0) / t_A^2(\omega_0)] . \quad (9)$$

Besides the measured current ratio, formula (9) involves only the one-photon cross section and, through  $Q$ , the refractive index and the nonlinear tensor coefficient  $\chi_{xxx}^{(2)}$ . This latter quantity is known from fairly accurate experiments.<sup>16–18</sup> The measurement does not require any knowledge of the fluorescence quantum yield nor of the properties of the collecting systems; also and most importantly, the value of  $\delta$  is free from any influence of the spatial and temporal structure of the laser beam. Note, however, that we have made the implicit assumption that the fluorescence quantum yield is the same for one- and two-photon excitation<sup>19</sup>: As a result the same calibrating coefficient  $C_A$  appears in Eqs. (5) and (7). This is rigorously justified if the same excited states are reached in both processes and should be a good assumption in most cases.

The conditions of validity of Eq. (3) for a beam of finite angular and frequency spreads can be stated simply. We give here only the physical considerations leading to them; a more detailed study can be found in the Appendix. Call  $\Delta\theta$  and  $\Delta\omega$  the angular and frequency half-width at half-power of the laser radiation and introduce the length  $r_c = \lambda_0 / 4\Delta\theta = \pi / 2k_0\Delta\theta$  and the time interval  $t_c = \pi / 2\Delta\omega$ . In the case of a statistical signal they can be defined, respectively, as the coherence radius on a transverse section of the beam and the coherence time. For a deterministic signal they give a measure of the transverse length and the time interval over which the amplitude and phase can vary appreciably.

When the fundamental beam propagates inside the crystal it creates a source nonlinear polarization, which in turn gives rise to a “homogeneous” and an “inhomogeneous” wave.<sup>20</sup> The Poynting vectors of the homogeneous harmonic wave and of the fundamental wave will generally have different directions. As a result the harmonic will tend to walk off from the fundamental beam, and harmonic intensity at point  $\vec{r}$  will receive contributions from the nonlinear polarization over various parts of the transverse area. This is the so-called aperture effect<sup>21</sup> which will cause a distortion of the transverse structure if the beam separation on the exit face is larger than  $r_c$ . This corresponds to condition (A17) of the Appendix.

Similarly, the homogeneous and inhomogeneous waves will propagate inside the platelet, respectively, with the fundamental and harmonic group velocity. These are generally different and a distortion will occur in the harmonic envelope if the difference in transit time is larger than  $t_c$ . This gives condition (A18).

Finally, it is essential in our reasoning that diffraction does not modify the transverse structure of the beams. More precisely if propagation occurs over a distance  $a$ , the diffraction spread  $a\Delta\theta$  must be smaller than  $r_c = \lambda_0 / 4\Delta\theta$ . This must, of course, be satisfied with  $a$  equal to the plate thickness for relation (4) to hold. This condition, which corresponds to (A19), is however not sufficient, it is also necessary that the integrals in the right-hand sides of Eqs. (5)–(8) preserve their values when the beams propagate from the platelet to the cells. This will certainly be the case if the corresponding distances are smaller than  $\lambda_0 / 4(\Delta\theta)^2$ . Although this condition is somewhat too restrictive owing to the averaging effect of spatial integration (note that the integral of  $F_2$ , which is the total harmonic flux, is of course invariant during the propagation), we shall have it satisfied in our experiments.

### III. THE EXPERIMENT

#### A. Experimental Setup

The ruby laser,  $Q$  switched by a rotating prism, had a power of about 40 MW and a pulse duration of about 40 nsec. Its total divergence was less than 1.5 mrad and its spectral width was reduced to less than  $0.06 \text{ cm}^{-1}$  by use of two parallel plates as an output mirror. The light was exactly vertically polarized by a Glan-Thomson prism. The unfocused laser beam was incident on a crystalline quartz plate 1.102 mm thick, oriented as shown in Fig. 3. We checked that the  $x$  axis was exactly parallel ( $\pm 5'$ ) to the polarization direction of the Glan prism with an auxiliary He-Ne laser. The laser created a vertically polarized second-harmonic beam, since in this case, the only component is

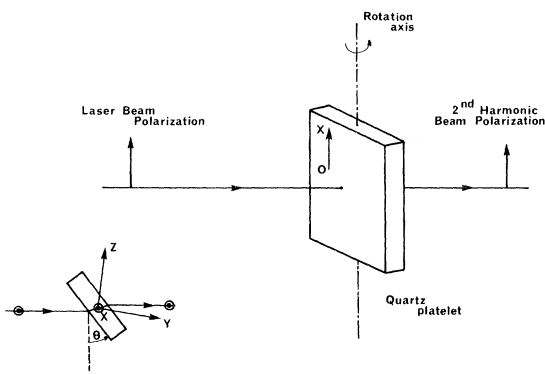


FIG. 3. Orientation of the (011) quartz slab used in the experiment.

$$P_x(2\omega, \vec{r}) = \chi_{xxx}^{(2)} E_x(\omega, \vec{r}) E_x(\omega, \vec{r}) .$$

First, as a preexperiment, we measured the second-harmonic intensity as a function of the orientation of the plate. From the Maker fringes (see Fig. 4) we deduced the coherence length of the quartz:

$$l_c = \lambda/4 |n_0^{2\omega} - n_0^\omega| = 6.85 \pm 0.02 \mu .$$

The orientation was adjusted to  $15^\circ 10'$  and was no longer changed. The experimental setup was then completed as shown in Fig. 5. The second-harmonic beam was collinear with the fundamental one and induced fluorescence in the solution which was contained in a 1-cm-thick cell. To reduce the influence of diffraction, this cell was placed

very close (3.5 cm) to the quartz plate, leaving space for a colored-glass filter between the cell and the plate.

The fluorescence of the solution was measured by detector  $D_A$ , a ten-stage 150 AVP radiotechnique photomultiplier (S4 photocathode). An interference filter and colored glasses were placed in front of the photomultiplier  $D_A$  to eliminate any stray light from the ruby or the second harmonic.

The use of a beam splitter plate is better avoided as it could introduce a distortion in the intensity distribution. The second harmonic reflected at the output face of the quartz plate was filtered with a  $\text{CuSO}_4$  cell and an interference filter and produced fluorescence in a cell containing the same solution as the other. This reference signal was measured by detector  $D_B$ , another 150 AVP photomultiplier, to ensure an identical time response, taking into account fluorescence lifetime. All the data (ruby, fluorescence signals) were automatically recorded by a processing system including analog to digital converters.

#### B. Experimental Procedure

There are 2 steps: (i) First, a uv filter (UG1 Schott, 2 mm) is put before the solution cell. By varying the calibrated neutral filters before the quartz and before the detectors  $D_A$  and  $D_B$ , the following curve is plotted:

$$I_A = F(I_B)$$

(see Fig. 6). (ii) In the second step, the uv filter is removed and a red glass (RG1 Schott) was inserted. Again, with the same technique, the curve

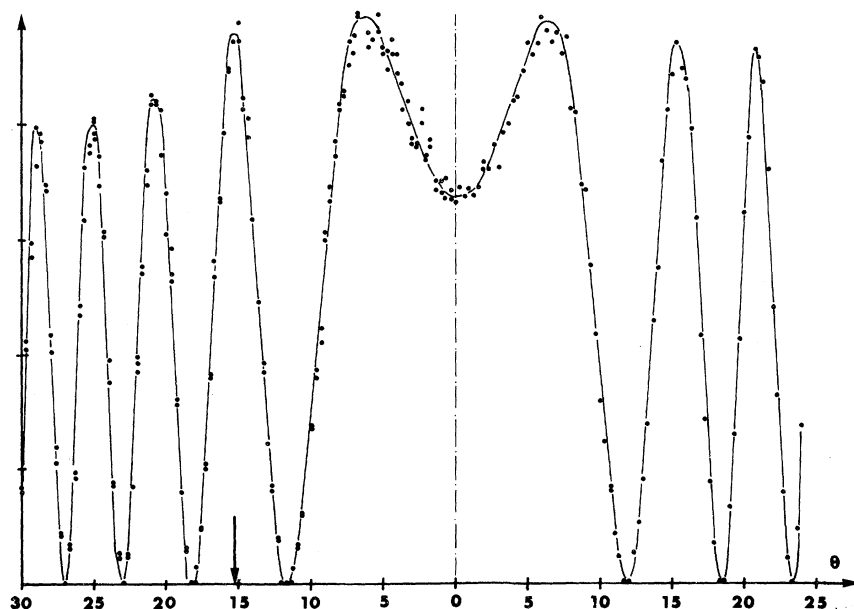


FIG. 4. Maker fringes; second-harmonic intensity (arbitrary units) vs slab orientation sample thickness 1.102 mm. Arrow indicates the chosen slab orientation.

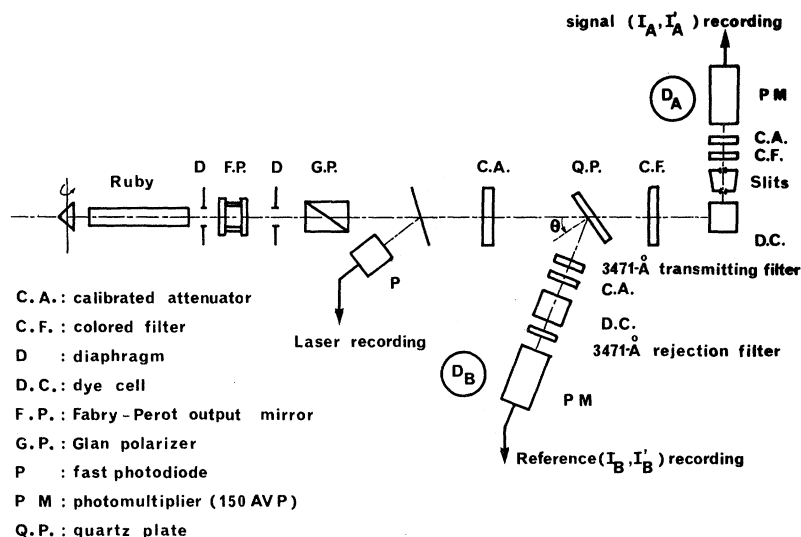


FIG. 5. Experimental setup for the measurement of the two-photon cross sections.

$$I'_A = F(I'_B)$$

is plotted (see Fig. 6).

In fact, one value of each couple ( $I_A, I_B$ ) and ( $I'_A, I'_B$ ) is sufficient to obtain the value of  $\delta$  [Eq. (9)], but the plotting of the curves yielded a check of the  $I_A$  vs  $I_B$  correlation and contributed to reduce the shot noise.

A further check is provided by the study of  $I_A$  and  $I'_A$  as function of the laser intensity; the exact quadratic variation which was observed in these cases proved that the measurements were free from any errors associated with self-focusing, saturation of the detectors, and stray-light detection.

#### C. Calibrations and Calculations

The value of  $\delta$  was directly obtained from Eq. (9). The calibrations of the filters were easy and accurate because they all worked on a very narrow spectral range and with a nearly parallel beam.  $\sigma$  was obtained from the literature or measured directly (see Table I).

#### D. Experimental Difficulties

To avoid errors, several precautions were taken.

*Stray light.* We shielded the cells against daylight and laser flash by putting them into boxes painted black and made sure there was no light coming in when the laser beam was absent.

*Burning.* This was the hardest problem to solve. We made sure there was no appreciable signal  $I_A$  when the cell was filled with the solvent without any dye. The signal/burning ratio was never less than 60. To get this result, we carefully purified the solvent with active carbon, to remove any dust from the liquid and especially from the cell windows. Then, we used two vertical slits arranged

so that no light coming from the windows could reach the "photomultiplier" (PM) photocathode. One slit had a width of 2 mm and was placed against

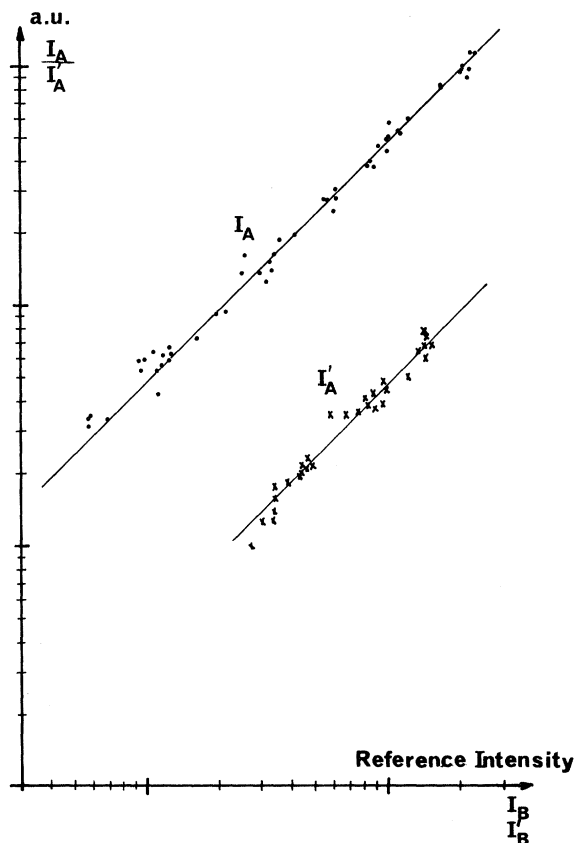


FIG. 6. Fluorescence intensity vs reference intensity (arbitrary units, log-log scale);  $I_A$  is the fluorescence due to two-photon absorption and  $I'_A$  is the fluorescence due to one-photon absorption of the second harmonic (dimethyl-POPOP in methyl-cyclohexane).

TABLE I. Two-photon absorption cross sections at 6943 Å.

Substance	Solvent	$\sigma$ at 3471 Å (cm <sup>2</sup> )	$\delta/ \chi^{(2)} ^2$	$\delta$ at 6943 Å cm <sup>4</sup> sec/photon
Anthracene	Cyclohexane	$1.22 \times 10^{-17}$ <sup>a</sup>	$(0.43 \pm 0.062) \times 10^{-33}$	$(0.23 \pm 0.1) \times 10^{-50}$
B. B. O. T.	Methylcyclohexane	$16.1 \times 10^{-17}$ <sup>a</sup>	$(7.5 \pm 1.4) \times 10^{-33}$	$(4 \pm 2) \times 10^{-50}$
Dimethyl-POPOP	Methylcyclohexane	$17.5 \times 10^{-17}$ <sup>a</sup>	$(21.6 \pm 2) \times 10^{-33}$	$(11.5 \pm 4.5) \times 10^{-50}$
4-methyl-7-diethylamino coumarin	Ethanol	$4.82 \times 10^{-17}$ <sup>b</sup>	$(27.1 \pm 3.5) \times 10^{-33}$	$(14.5 \pm 6) \times 10^{-50}$

<sup>a</sup>Reference 26.<sup>b</sup>Direct measurement (Cary 14 spectrophotometer).

the side of the cell, at its center. The other slit had a width of 4 mm and was placed against the photocathode. Thus, the solid angle and the active volume were well defined.

A consequence of the presence of these slits was that we looked only at the central part of the cell. Since the transmission of the 1-cm cell was 50% at 3471 Å, we corrected the transmission  $t_A(2\omega_0)$  for the absorption in the first millimeters of the cell.

#### IV. RESULTS AND DISCUSSION

##### A. Results and Accuracy

The results obtained by the present method on four different molecules in solutions and for ruby-laser irradiation ( $\lambda = 6943$  Å) are shown in Table I. The values of  $\delta$  were determined from Eq. (9) where the coefficient  $Q$  was calculated from Eq. (A22) with the following values of the linear and nonlinear constants of quartz:

$$n_0^{(\omega)} = n_s = 1.54068,$$

$$n_0^{(2\omega)} = n_F = 1.56608,$$

$$\chi_{xxx}^{(2)} = 2.3 \times 10^{-9} \text{ esu } (\pm 20\%).$$

The latter value is obtained from the absolute measurement

$$\chi_{xxx}^{(2)}(\text{LiIO}_3) = 36 \times 10^{-9} \text{ esu } (\pm 15\%)$$

by Cappillo and Tang,<sup>17</sup> and the relative measurement

$$\chi_{xxx}^{(2)}(\text{LiIO}_3) = 15.5 \times \chi_{xxx}^{(2)}(\text{quartz}) (\pm 5\%)$$

by Jerphagnon.<sup>18</sup> This value is recommended by Bechmann and Kurtz<sup>22</sup> and Jerphagnon.<sup>23</sup> These yield a value of  $Q$ :

$$Q = (1.06 \pm 0.4) \times 10^{-34} \text{ cm}^2 \text{ sec.}$$

The relative accuracy of the results varies slightly from one substance to the other and is about  $\pm 50\%$ . There are four main sources of errors: (i) the determination of the one-photon cross section  $\sigma$  contributing  $\pm 4\%$ ; (ii) shot noise introducing in the measurement of the current ratio

$I'_A/I_A$  a relative error around  $\pm 5\%$ ; (iii) the measurement of the filter transmissions giving an error  $\pm 7\%$  for the ratio  $t_A(2\omega_0)/t_A^2(\omega_0)$ ; (iv) the uncertainty  $\pm 20\%$  in the value of  $\chi_{xxx}^{(2)}$  which, we recall, is obtained from a relative plus an absolute measurement.

These determinations of  $\delta$  were made several times with different ruby rods, quartz samples, and photomultipliers; the results were reproducible within the measurement uncertainties.

*Sensitivity of this method.* With the present experimental arrangement, we can get a sufficient signal for molecules for which the fluorescence quantum yield  $\eta$  is such that

$$\eta \delta \geq 0.005 \times 10^{-50} \text{ cm}^4 \text{ sec/photon and } \eta \geq 0.01.$$

This latter condition could be relaxed by using a substance more nonlinear than quartz.

##### B. Comparison with Other Works

We have summarized on Table II the results obtained by various authors using different versions of the fluorescence method for the anthracene molecule in solution ( $\lambda_0 = 6943$  Å). The values exhibit a very large scatter which can be attributed to errors in the calibration of the detection channel or irregularities in the laser structure. It is gratifying to notice that the results closest to those of the present work are those of the authors<sup>10</sup> who have taken the greatest care in eliminating these two main sources of errors.

Topp and Rentzepis<sup>24</sup> have determined  $\delta$  for dimethyl-POPOP in methylcyclohexane, by measuring the gain produced by two-photon pumping by a mode-locked ruby laser. From this, they estimated the population created in the upper singlet state and a value of  $\delta = 200 \times 10^{-50} \text{ cm}^4 \text{ sec/photon}$ , which is 17 times larger than that obtained in the present work. Such a gain measurement is of course free from errors associated with the calibration of the detecting channel: It requires only relative intensity measurements. It is however strongly influenced by the spatial distribution of the density of excited molecules and of the flux density of the probing beam. Furthermore, an accu-

TABLE II. Results obtained from the fluorescence in anthracene.

Author	Solvent	Calibration of laser	Calibration of detection	Result in $10^{-50} \text{ cm}^4 \text{ sec}$
Peticolas <i>et al.</i> (Ref. 27)	EPA glass	Calorimeter	CW spectral lamp	0.09
Galanin and Chizhikova (Ref. 9)	Ethanol	Calorimeter	Flash lamp + calorimeter	1.75
Aleksandrov <i>et al.</i> (Ref. 28)		Calorimeter	Photometric lamp	0.6
Webman and Jortner (Ref. 29)	Benzene	Comparison with a two-beam method and ratio crystal/solution		0.005
Aleksandrov and Bredikhin (Ref. 10)	Cyclohexane	Calorimeter + photograph	Second harmonic + calorimeter + photograph	$0.16 \pm 0.05$
Our work	Cyclohexane	Not necessary	Not necessary	$0.23 \pm 0.1$

rate knowledge of the flux density of the exciting beam is also required to deduce  $\delta$  from the number of excited molecules. Thus, the measured value will be very sensitive to the coherence properties of the beams. These properties, as is well known, are particularly difficult to determine for real mode-locked lasers.

We have performed a direct two-photon absorption measurement of  $\delta$  for 4-methyl-7-diethylamino coumarin. The transmitted flux  $F(l)$  of a ruby-laser beam passed through a concentrated solution in acetone (1 mole/liter) was studied as a function of the incident flux  $F(0)$ . A straightforward analysis gives for the expected variation

$$F(l) = F(0) e^{-\alpha l} \{1 + [2\delta N F(0)/\alpha] (1 - e^{-\alpha l})\}^{-1},$$

where  $\alpha$  is the linear extinction coefficient. This variation was observed experimentally and yielded a value  $\delta = 50 \times 10^{-50} \text{ cm}^4 \text{ sec/photon}$ . This value is about three times larger than that obtained in this work. It should be kept in mind that it is affected by our imperfect knowledge of the coherent properties of the beam and also by the formation of molecular aggregates which can occur at such high concentrations.

## V. CONCLUSION

In conclusion, let us summarize the main characteristic features of the method proposed in this paper:

First, it exhibits the general shortcoming of fluorescence methods. Although this method does not require a determination of the fluorescence quantum yield, it relies on the assumption that the fluorescence is the same for one- and two-photon excitation. This difficulty, however, is not considered to be serious when only one excited electronic

state is involved in the process.

No calibration of the detecting channel is required. This improves the accuracy of the measurement. This accuracy is limited at the present time by that of the absolute measurements of  $\chi_{xxx}^{(2)}$ . Improvements in this respect are to be expected.

The measured value of  $\delta$  is free from any influence of the spatial and temporal coherence properties of the laser beam. We believe this last point to be particularly important, as an accurate control of the coherence properties is fairly difficult with the high peak power lasers required for these experiments.

## ACKNOWLEDGMENTS

Dr. J. Jerphagnon kindly tested our quartz plate. Several very fruitful discussions with him and Dr. A. Mysyrowicz are gratefully acknowledged, as well as the assistance provided throughout the experiment by R. Clement and J. Debric.

## APPENDIX

In this Appendix we study the validity conditions of Eq. (4). We determine the upper limits on the angular and frequency spreads and give an explicit expression for the coefficient  $Q$  relating the fundamental and harmonic fluxes.

Consider the harmonic generation due to a fundamental light beam propagating through a nonlinear parallel slab immersed in air (Fig. 7). The light beam is polarized along the  $X$  axis (unit vector  $\hat{x}$ ), normal to the plane of incidence, inside and outside the slab. The orientation of the crystal axes is such that this polarization is that for an ordinary wave propagating in the figure ( $yz$ ) plane. The corresponding frequency-dependent refractive index is  $n(\omega)$ . The fundamental electric field in the incident

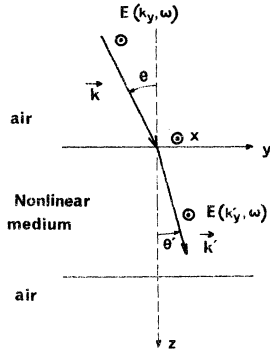


FIG. 7. Refraction of light at the entrance of a nonlinear material.

half-space is represented by

$$\vec{E}(\vec{r}, t) = \hat{x} E(\vec{r}, t) e^{i(\vec{k}_0 \cdot \vec{r} - \omega_0 t)} + \text{c. c.},$$

where  $E(\vec{r}, t)$  is a complex envelope function which accounts for the finite angular and frequency spreads and can be expressed as

$$E(\vec{r}, t) = \int_{-\infty}^{+\infty} dk_y \int_{-\infty}^{+\infty} d\omega E(k_y, \omega) \times \exp[i[(\vec{k} - \vec{k}_0) \cdot \vec{r} - (\omega - \omega_0)t]]. \quad (\text{A1})$$

Here  $k_y$  is the projection on the plane of the slab of the wave vector  $\vec{k}$  with modulus  $k = \omega/c$ . For the sake of simplicity we have considered the angular spread to be in the  $yz$  plane only and reduced the problem to a two-dimensional one. With this expression

$$\vec{E}(\vec{r}, t) = \hat{x} \int_{-\infty}^{+\infty} dk_y \int_{-\infty}^{+\infty} d\omega E(k_y, \omega) e^{i(\vec{k} \cdot \vec{r} - \omega t)} + \text{c. c.} \quad (\text{A2})$$

We assume the angular and frequency spreads to be small around the mean values  $\vec{k}_0$  and  $\omega_0$ . More specifically we assume that, for all practical purposes  $E(k_y, \omega) = 0$  when  $|k_y - k_{y0}| > \Delta k_y$ ,  $|\omega - \omega_0| > \Delta\omega$  with  $\Delta k_y \ll k_0$ ,  $\Delta\omega \ll \omega_0$ .

The fundamental field inside the crystal creates a nonlinear source polarization which in turn produces an harmonic field. We want to determine this harmonic field on the exit face of the slab. Bloembergen and Pershan<sup>20</sup> have solved this problem for a parallel plate with perfectly plane faces, taking into account the reflections of the fundamental field inside the plate. As noted by Jerphagnon and Kurtz,<sup>15</sup> this does not give an appropriate description of experiments performed with a roughly polished plate. In such a case the interferences between successive reflected waves tend to average out: The plate constitutes an interferometer with poor discrimination. This corresponds to our experimental situation and our treatment will parallel that of Jerphagnon and Kurtz: The boundary conditions at  $z = 0$  and  $z = L$  are applied independently.

The first set determines the forward propagating harmonic field inside the crystal, the second one the harmonic field in the exit half-space.

Call  $\vec{E}'(\vec{r}, t)$  the fundamental field *inside* the plate,

$$\vec{E}'(\vec{r}, t) = \hat{x} \int_{-\infty}^{+\infty} dk_y \int_{-\infty}^{+\infty} d\omega E'(k_y, \omega) \times e^{i(\vec{k}' \cdot \vec{r} - \omega t)} + \text{c. c.},$$

where  $k'_y = k_y$ , and  $E'(k_y, \omega)$  and  $E(k_y, \omega)$  are simply related by Fresnel's formula<sup>25</sup>

$$E'(k_y, \omega) = \frac{2 \cos \theta}{n(\omega) \cos \theta + \cos \theta'} E(k_y, \omega) = t(k_y, \omega) E(k_y, \omega), \quad (\text{A3})$$

where  $\theta$  and  $\theta'$  are the angles with the slab normal made, respectively, by the wave vectors  $\vec{k}$  and  $\vec{k}'$ . Ignoring in the present experimental situation the dispersion of the nonlinear tensor  $\chi^{(2)}$ , the source nonlinear polarization  $\vec{P}_{\text{NLS}}(\vec{r}, t)$  inside the medium is given by

$$\vec{P}_{\text{NLS}}(\vec{r}, t) = \vec{p}_{\text{NLS}}(\vec{r}, t) e^{i(2\vec{k}_0 \cdot \vec{r} - 2\omega_0 t)} + \text{c. c.},$$

with

$$\vec{p}_{\text{NLS}}(\vec{r}, t) = \chi^{(2)} \hat{x} \hat{x} E'(\vec{r}, t) E'(\vec{r}, t). \quad (\text{A4})$$

The source polarization appears as a sum of terms, each corresponding to a pair of wave vectors and frequencies  $(\vec{k}'_1, \omega_1)$   $(\vec{k}'_2, \omega_2)$ . We now proceed to determine the harmonic field created by the source polarization corresponding to such a pair:

$$\begin{aligned} \vec{P}_{\text{NLS}}(\vec{r}, t; \vec{k}'_1, \omega_1; \vec{k}'_2, \omega_2) &= \vec{P}_{\text{NLS}}(\vec{r}, t; 1; 2) \\ &= \chi^{(2)} \hat{x} \hat{x} E'(k_{1y}, \omega_1) E'(k_{2y}, \omega_2) \\ &\quad \times \exp[i[(\vec{k}'_1 + \vec{k}'_2) \cdot \vec{r} - (\omega_1 + \omega_2)t]] \\ &= \vec{p}_{\text{NLS}}(1; 2) \exp[i[(\vec{k}'_1 + \vec{k}'_2) \cdot \vec{r} - (\omega_1 + \omega_2)t]]. \quad (\text{A5}) \end{aligned}$$

For the sake of simplicity we take  $\vec{p}_{\text{NLS}}$  normal to the plane of incidence. Thus it will also generate an ordinary harmonic wave. This corresponds to the experimental situation described in the text. The geometry and notation are shown on Fig. 8. The expression for the sum frequency field is directly obtained from Bloembergen and Pershan's work<sup>20</sup> as

$$\begin{aligned} \vec{E}'_H(\vec{r}, t; 1; 2) &= \frac{-4\pi \vec{p}_{\text{NLS}}(1; 2)}{n_F^2 - n_S^2} e^{-i(\omega_1 + \omega_2)t} \\ &\quad \times \left[ e^{i\vec{k}'_S \cdot \vec{r}} - \left( \frac{n_S \cos \theta'_S + \cos \theta_R}{n_F \cos \theta'_F + \cos \theta_R} \right) e^{i\vec{k}'_F \cdot \vec{r}} \right]. \quad (\text{A6}) \end{aligned}$$

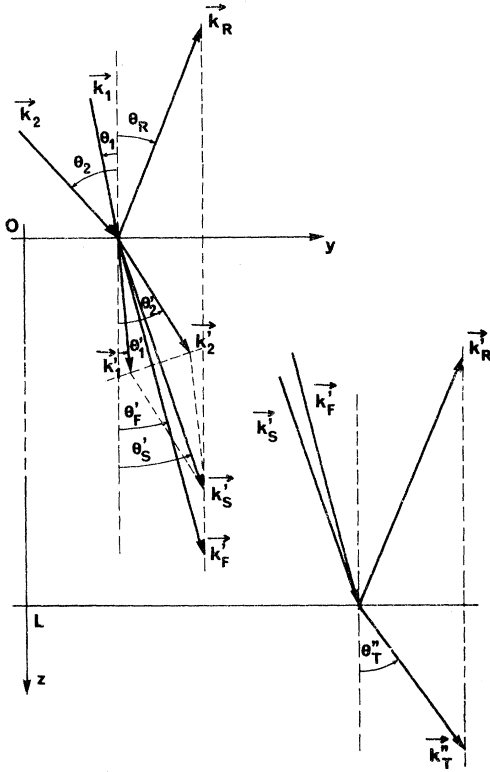


FIG. 8. Fundamental and harmonic waves in the non-linear material. The indexes 1 and 2 designate two laser waves, F the "free" harmonic wave, S the "source" harmonic wave, R and T the reflected and transmitted waves at a boundary.

In this expression  $\vec{k}'_S = \vec{k}'_1 + \vec{k}'_2$  is the wave vector of the inhomogeneous ("source") component of the sum frequency wave, and  $\vec{k}'_F$  is that corresponding to the homogeneous ("free") wave

$$n_F = n(\omega_1 + \omega_2) \quad \text{and} \quad |\vec{k}'_F| = n_F \frac{\omega_1 + \omega_2}{c} . \quad (\text{A7})$$

The continuity conditions at  $z=0$  require that

$$k_{1y} = k'_{1y}, \quad k_{2y} = k'_{2y},$$

$$k'_{Fy} = k'_{Sy} = k'_{1y} + k'_{2y} = k_{1y} + k_{2y} .$$

The effective refractive index for the source component,  $n_S$ , is defined in such a way that

$$\begin{aligned} \frac{n_S \sin \theta'_S (\omega_1 + \omega_2)}{c} &= k'_{Fy} = k'_{Sy} \\ &= \frac{n(\omega_1) \omega_1 \sin \theta'_1 + n(\omega_2) \omega_2 \sin \theta'_2}{c} \end{aligned}$$

or

$$n_S (\omega_1 + \omega_2) / c = |\vec{k}'_S| . \quad (\text{A8})$$

The angle  $\theta_R$  is that made with the plate normal by the sum-frequency reflected wave in the incidence half-space deduced from the continuity condition

$$k_{Ry} = \frac{\omega_1 + \omega_2}{c} \sin \theta_R = k_{1y} + k_{2y} . \quad (\text{A9})$$

To obtain the sum-frequency field in the exit half-space we use the boundary conditions at  $z=L$  where the tangential components of the electric and magnetic fields must be continuous. To satisfy these conditions we introduce the reflected sum-frequency field

$$\vec{E}'_{HR}(\vec{r}, t; 1; 2) = \hat{x} E'_{HR} e^{iL\vec{k}'_R \cdot \vec{r} - (\omega_1 + \omega_2)t} ,$$

with

$$k'_{Ry} = k'_{Fy} = k'_{Sy}, \quad k'_{Rx} = -k'_{Fx}, \quad (\text{A10})$$

and the transmitted sum-frequency field in the exit half-space

$$\vec{E}''_H(\vec{r}, t; 1; 2) = \hat{x} E''_H e^{iL\vec{k}''_T \cdot \vec{r} - (\omega_1 + \omega_2)t} ,$$

with  $\vec{k}''_T$  again determined by the continuity conditions

$$k''_{Ty} = k'_{Fy} = k'_{Sy} \quad \text{and} \quad |\vec{k}''_T| = (\omega_1 + \omega_2) / c . \quad (\text{A11})$$

When the magnetic fields are calculated from Maxwell's equation for a nonmagnetic medium

$$\vec{\nabla} \times \vec{E} = -\frac{1}{c} \frac{\partial \vec{H}}{\partial t} = i \frac{\omega_1 + \omega_2}{c} \vec{H} ,$$

the boundary conditions take the following form:

$$\begin{aligned} -4\pi \frac{\vec{p}_{NLS}(1; 2)}{n_F^2 - n_S^2} \left[ e^{ik_S z L} - \left( \frac{n_S \cos \theta'_S + \cos \theta_R}{n_F \cos \theta_F + \cos \theta_R} \right) e^{ik'_F z L} \right] \\ + E'_{HR} e^{-ik'_F z L} = E''_H e^{ik''_T z L} \end{aligned}$$

and

$$\begin{aligned} -4\pi \frac{\vec{p}_{NLS}(1; 2)}{n_F^2 - n_S^2} \left[ n_S \cos \theta'_S e^{ik_S z L} - \left( \frac{n_S \cos \theta'_S + \cos \theta_R}{n_F \cos \theta_F + \cos \theta_R} \right) \right. \\ \left. \times n_F \cos \theta'_F e^{ik'_F z L} \right] - n_F \cos \theta'_F E'_{HR} e^{-ik'_F z L} \\ = E''_H \cos \theta''_T e^{ik''_T z L} , \end{aligned}$$

from which one obtains

$$\vec{E}''_H(\vec{r}, t; 1; 2) = -4\pi \frac{\vec{p}_{NLS}(1; 2)}{n_F^2 - n_S^2} \left[ \left( \frac{n_F \cos \theta'_F + n_S \cos \theta'_S}{n_F \cos \theta_F + \cos \theta_R} \right) e^{ik'_F z L} \right]$$

$$-\frac{2n_F \cos\theta'_F}{n_F \cos\theta'_F + \cos\theta''_F} \left( \frac{n_S \cos\theta'_S + \cos\theta_R}{n_F \cos\theta'_F + \cos\theta_R} \right) e^{ik'_F z L} \left] \exp i[k'_y y + k''_z(z-L) - (\omega_1 + \omega_2)t]. \quad (\text{A12})$$

The total harmonic field  $\vec{E}''_H(\vec{r}, t)$  is obtained by summing over all the different pairs (1; 2):

$$\vec{E}''_H(\vec{r}, t) = \iint_{-\infty}^{+\infty} dk_{y1} dk_{y2} \iint_{-\infty}^{+\infty} d\omega_1 d\omega_2 \times \vec{E}''_H(\vec{r}, t; 1; 2) + \text{c. c.} \quad (\text{A13})$$

When far from a phase-matching direction, the variations with angle and frequency come predominantly from the phase terms in (A12). To be specific for the quartz slab used in our experiments

(see Sec. III),

$$\frac{\partial n_F}{\partial \omega} = 12.3 \times 10^{-8} \text{ sec}, \quad \frac{\partial n_S}{\partial \omega} = 6.5 \times 10^{-8} \text{ sec}, \\ \theta'_F \approx \theta'_S \approx 0.17, \quad \theta_R \approx \theta'' \approx 0.26,$$

and for the laser beam,  $\Delta\omega \lesssim 0.06 \text{ cm}^{-1}$  and  $\Delta\theta \approx 0.75 \text{ mrad}$ . The coefficients of the exponentials inside the brackets will vary for all possible pairs by at most a few parts in a thousand. Furthermore the difference between these coefficients is

$$\frac{n_F \cos\theta'_F + n_S \cos\theta'_S}{n_F \cos\theta'_F + \cos\theta''_F} - \frac{2n_F \cos\theta'_F}{n_F \cos\theta'_F + \cos\theta''_F} \left( \frac{n_S \cos\theta'_S + \cos\theta_R}{n_F \cos\theta'_F + \cos\theta_R} \right) \\ = \frac{n_F \cos\theta'_F - n_S \cos\theta'_S}{n_F \cos\theta'_F + \cos\theta''_F} \left( \frac{n_F \cos\theta'_F - \cos\theta_R}{n_F \cos\theta'_F + \cos\theta_R} \right) \approx (n_F - n_S) \frac{n_F - 1}{(n_F + 1)^2} \lesssim 10^{-3}.$$

These variations and differences will be neglected here, as well as the variations of the Fresnel factors  $t(\vec{k}, \omega)$  given in (A3). Using (A12), (A13), and taking into account the expression (A5) of  $\vec{p}_{\text{NLS}}(1; 2)$  we obtain

$$\vec{E}''_H(\vec{r}, t) \approx \hat{x} A \iint_{-\infty}^{+\infty} dk_{y1} dk_{y2} \iint_{-\infty}^{+\infty} d\omega_1 d\omega_2 \\ \times \chi_{xzx}^{(2)} E(k_{y1}, \omega_1) E(k_{y2}, \omega_2) \\ \times \sin\psi(1; 2) \exp \left[ i \left( \frac{k_{Sx} + k_{Fx}}{2} \right) L \right] \\ \times \exp i[k'_y y + k''_z(z-L) - (\omega_1 + \omega_2)t] + \text{c. c.}, \quad (\text{A14})$$

where the quantity

$$A = -8\pi i \left( \frac{1}{n_F^2 - n_S^2} \right) \left( \frac{n_F \cos\theta'_F + n_S \cos\theta'_S}{n_F \cos\theta'_F + \cos\theta''_F} \right) \\ \times t(\vec{k}_1, \omega_1) t(\vec{k}_2, \omega_2)$$

is evaluated for  $\vec{k}_1 = \vec{k}_2 = \vec{k}_0$  and  $\omega_1 = \omega_2 = \omega_0$ , and

$$\psi(1; 2) = (k'_{Sx} - k'_{Fx})(L/2) \\ = (n_S \cos\theta'_S - n_F \cos\theta'_F)(\omega_1 + \omega_2)(L/2c). \quad (\text{A15})$$

We now consider the variation of  $\psi$  with the pair (1; 2). Using the definition (A7) for  $n_F$  and (A8) for  $n_S$

$$\psi(1; 2) = \frac{1}{2} L \{ [k'^2_F - (k'_{y1} + k'_{y2})^2]^{1/2} \\ - (k'^2_1 - k'^2_{y1})^{1/2} - (k'^2_2 - k'^2_{y2})^{1/2} \} \\ = \psi(0; 0) + \delta\omega_1 \frac{\partial \psi}{\partial \omega_1} + \delta\omega_2 \frac{\partial \psi}{\partial \omega_2} \\ + \delta k_{y1} \frac{\partial \psi}{\partial k_{y1}} + \delta k_{y2} \frac{\partial \psi}{\partial k_{y2}} + \dots,$$

where the derivatives are evaluated for  $\vec{k}_1 = \vec{k}_2 = \vec{k}_0$  and  $\omega_1 = \omega_2 = \omega_0$ ;

$$\psi(1; 2) = \frac{L}{2} (k'_{Fz0} - k'_{Sx0}) + L \left( \frac{1}{v_{zF}^0 \cos\theta'_{F0}} - \frac{1}{v_{zS}^0 \cos\theta'_{S0}} \right) \frac{\delta\omega_1 + \delta\omega_2}{2} \\ + L (\tan\theta'_{S0} - \tan\theta'_{F0}) \frac{\delta k_{y1} + \delta k_{y2}}{2} + L \left( \frac{\partial |k'_f|}{\partial k_{Fy}} \Big|_0 - \frac{\partial |k'_f|}{\partial k_y} \Big|_0 \right) \frac{1}{\cos\theta'_{F0}} - \frac{1}{\cos\theta'_{S0}} \\ \times \frac{\delta k_{y1} + \delta k_{y2}}{2} + \frac{L}{2} \frac{(\delta k_{y1})^2 + (\delta k_{y2})^2}{2} \left( \frac{1}{k'_{S0} \cos^3\theta'_{S0}} - \frac{1}{k'_{F0} \cos\theta'_{F0}} \right) - \frac{L}{2} \delta k_{y1} \delta k_{y2} \frac{1}{k'_{F0} \cos^3\theta'_{F0}}. \quad (\text{A16})$$

In our experimental situation the anisotropy terms  $\partial|\vec{k}|/\partial k_y$ , which express the variation of the refractive index with the direction of propagation, are absent since both fundamental and harmonic waves propagate in the ordinary mode.

At the top of a Maker fringe  $\psi(0; 0) = (2m + 1)\frac{1}{2}\pi$  and  $\sin\psi(1; 2) \approx 1 - \frac{1}{2}(\delta\psi)^2$  will be negligibly affected by the angular and frequency variations as long as  $\delta\psi$  is less than some limit that we arbitrarily equal to  $\frac{1}{10}\pi$ . This gives the conditions

$$\Delta k_y = k_0 \Delta\theta \cos\theta_0 \leq \frac{\pi}{10} \frac{1}{L(\tan\theta'_{S_0} - \tan\theta'_{F_0})}, \quad (\text{A17})$$

$$\Delta\omega \leq \frac{\pi}{10} \frac{v_{gF}^0 v_{gS}^0 \cos\theta'_{F_0} \cos\theta'_{S_0}}{L(v_{gF}^0 \cos\theta'_{F_0} - v_{gS}^0 \cos\theta'_{S_0})}, \quad (\text{A18})$$

for the first-order terms.

Since the incidence angle  $\theta_0$  can be small, (A17) can be satisfied even for a fairly divergent beam.

In this case, it becomes necessary to consider also the second-order terms in  $\delta k_y$ , which yield the condition

$$\Delta k_y = \cos\theta_0 k_0 \Delta\theta \leq \left( \frac{\pi k'_{S_0} \cos^3\theta_{S_0}}{5L} \right)^{1/2}. \quad (\text{A19})$$

The interpretation of conditions (A17)–(A19) has been given in the text. For the crystal geometry used in the present experiment they require

$$\Delta k_y \leq 330 \text{ cm}^{-1} \text{ from (A17),}$$

$$\Delta k_y \leq 700 \text{ cm}^{-1} \text{ from (A19),}$$

$$\Delta\omega \leq 10^{12} \text{ sec}^{-1} \text{ from (A18).}$$

In the experiment, we had  $\Delta k_y = 16 \text{ cm}^{-1}$  and  $\Delta\omega \leq 10^{10} \text{ sec}^{-1}$ .

Assuming these conditions are satisfied, then from (A14)

$$\begin{aligned} \vec{E}'_H(y, L, t) = \hat{x}A \sin\psi(0; 0) \iint_{-\infty}^{+\infty} dk_{y1} dk_{y2} \iint_{-\infty}^{+\infty} d\omega_1 d\omega_2 \chi_{xxx}^{(2)} E(k_{y1}, \omega_1) \\ \times E(k_{y2}, \omega_2) \exp i \left( \frac{k'_{S_z} + k'_{F_z}}{2} \right) L \exp i [(k_{y1} + k_{y2})y - (\omega_1 + \omega_2)t] + \text{c. c.}; \end{aligned}$$

or, expressing  $k'_{S_z}$  and  $k'_{F_z}$  as functions of  $k_{y1}$  and  $k_{y2}$ ,  $\omega_1$  and  $\omega_2$ ,

$$\begin{aligned} k'_{F_z} + k'_{S_z} &= [k_F'^2 - (k'_{y1} + k'_{y2})^2]^{1/2} + (k_1'^2 - k_{y1}'^2)^{1/2} + (k_2'^2 - k_{y2}'^2)^{1/2} \\ &= (k_{Fz}^0 + k_{S_z}^0) + \frac{1}{k'_{Fz}} \left( k'_f \frac{\partial k'_f}{\partial \omega} (\omega_1 + \omega_2 - 2\omega_0) - k'_{Fy} (k'_{y1} + k'_{y2} - 2k'_{y0}) \right) \\ &\quad + \frac{1}{k'_{S_z}} \left( k'_s \frac{\partial k'_s}{\partial \omega} (\omega_1 + \omega_2 - 2\omega_0) - k'_{Sy} (k'_{y1} + k'_{y2} - 2k'_{y0}) \right) \\ &\approx \frac{1}{\cos\theta_{F_0}} \left( \frac{n_F}{c} - \frac{1}{v_{gF}} \right) 2\omega_0 + \frac{1}{\cos\theta_{S_0}} \left( \frac{n_S}{c} - \frac{1}{v_{gS}} \right) 2\omega_0 + (\omega_1 + \omega_2) \left( \frac{1}{v_{gF} \cos\theta_{F_0}} + \frac{1}{v_{gS} \cos\theta_{S_0}} \right) \\ &\quad - (k'_{y1} + k'_{y2}) (\tan\theta_{F_0} + \tan\theta_{S_0}) + O(k_{y0}'^2), \end{aligned}$$

one obtains

$$\begin{aligned} \vec{E}'_H(y, L, t) = \hat{x}A \sin\psi(0, 0) \exp \left\{ i \omega_0 L \left[ \frac{1}{\cos\theta_{F_0}} \left( \frac{n_F}{c} - \frac{1}{v_{gF}} \right) + \frac{1}{\cos\theta_{S_0}} \left( \frac{n_S}{c} - \frac{1}{v_{gS}} \right) \right] \right\} \\ \times \iint_{-\infty}^{+\infty} dk_{y1} dk_{y2} \iint_{-\infty}^{+\infty} d\omega_1 d\omega_2 \chi_{xxx}^{(2)} E(k_{y1}, \omega_1) E(k_{y2}, \omega_2) \exp i [(k_{y1} + k_{y2})(y - \Delta y) - (\omega_1 + \omega_2)(t - \Delta t)] + \text{c. c.}, \end{aligned} \quad (\text{A20})$$

where

$$\Delta y = L \frac{\tan\theta_{S_0} + \tan\theta_{F_0}}{2},$$

$$\Delta t = \frac{L}{2} \left( \frac{1}{v_{gF} \cos\theta_{F_0}} + \frac{1}{v_{gS} \cos\theta_{S_0}} \right)$$

are translation and retardation terms introduced by the propagation inside the slab. Remembering

the definition given in (A1), we deduce the modulus of the harmonic envelope:

$$|\vec{E}''_H(y, L, t)| = A \sin\psi(0; 0) \chi_{xxx}^{(2)} E^2(y - \Delta y, 0, t - \Delta t).$$

The harmonic flux density coming out of the crystal is

$$F_2(y, L, t) = \frac{c}{4\pi\hbar\omega_0} |\vec{E}''_H(y, L, t)|^2$$

$$= \frac{\pi \hbar \omega_0}{c} |A|^2 |\chi_{xxx}^{(2)}|^2 \times \sin^2 \psi F_1^2(y - \Delta y, 0, t - \Delta t). \quad (\text{A21})$$

The harmonic flux density at point  $y$  on the exit face and at time  $t$  is, within this approximation, proportional to the square of the fundamental flux density on the entrance face at point  $y - \Delta y$  and time  $t - \Delta t$ . This result holds whenever conditions (A17)–(A19) are satisfied. In the present case the retardation  $\Delta t$  and the translation  $\Delta y$  due to beam refraction are very small  $\Delta t = 2$  psec,  $\Delta y = 0.02$  cm and can be neglected. We obtain thus the result used in the

text, Eq. (4), with

$$Q = 64 \pi^3 \frac{\hbar \omega_0}{c} \frac{(\chi_{xxx}^{(2)})^2}{(n_F^2 - n_S^2)^2} \times \left( \frac{n_F \cos \theta'_F + n_S \cos \theta'_S}{n_F \cos \theta'_F + \cos \theta'_T} \right)^2 t^4 (\vec{k}_0, \omega_0). \quad (\text{A22})$$

This expression is, within the approximations made here, completely equivalent to that obtained for a monochromatic plane wave by Jerphagnon and Kurtz.<sup>15</sup> (Note that  $\chi_{xxx}^{(2)}$  is twice the nonlinear constant  $d_{11}$  used by these authors.)

<sup>14</sup>W. Kaiser and C. G. B. Garrett, Phys. Rev. Letters **7**, 229 (1961).

<sup>2</sup>For a review of experimental work on two-photon spectroscopy, see: J. M. Worlock, in *Laser Handbook*, edited by E. O. Schulz-DuBois and F. T. Arecchi (to be published).

<sup>3</sup>P. P. Sorokin and M. Braslau, IBM J. Res. Develop. **8**, 177 (1964).

<sup>4</sup>J. A. Giordmaine and J. A. Howe, Phys. Rev. Letters **11**, 207 (1963).

<sup>5</sup>S. Singh and J. E. Geusic, Phys. Rev. Letters **17**, 865 (1966).

<sup>6</sup>E. Panizza and P. J. Regensburger, Phys. Letters **24A**, 321 (1967).

<sup>7</sup>D. Fröhlich and H. Mahr, Phys. Rev. Letters **16**, 895 (1966).

<sup>8</sup>W. L. Peticolas, J. P. Goldsborough, and K. E. Rieckhoff, Phys. Rev. Letters **10**, 43 (1963).

<sup>9</sup>M. D. Galanin and Z. A. Chizhikova, Zh. Eksperim. i Teor. Fiz. Pis'ma v Redaktsiyu **4**, 41 (1966) [Sov. Phys. JETP Letters **4**, 27 (1966)].

<sup>10</sup>A. P. Aleksandrov and V. I. Bredikhin, Opt. i Spektroskopiya **30**, 72 (1971) [Sov. Phys. Opt. Spectry. **30**, 37 (1971)].

<sup>11</sup>J. Ducuing and N. Bloembergen, Phys. Rev. **133A**, 1473 (1964).

<sup>12</sup>J. Ducuing and J. A. Armstrong, in *Proceedings of the Third Conference on Quantum Electronics, Paris, 1963*, edited by N. Bloembergen and P. Grivet (Dunod, Paris, 1963).

<sup>13</sup>S. A. Akhmanov, A. I. Kovrigin, A. S. Chirkin, and O. N. Chunaev, Zh. Eksperim. i Teor. Fiz. **50**, 829 (1966) [Sov. Phys. JETP **23**, 549 (1966)].

<sup>14</sup>P. D. Maker, R. W. Terhune, M. Nisenoff, and C. M. Savage, Phys. Rev. Letters **8**, 21 (1962).

<sup>15</sup>J. Jerphagnon and S. K. Kurtz, J. Appl. Phys. **41**, 1667 (1970).

<sup>16</sup>J. Jerphagnon and S. K. Kurtz, Phys. Rev. B **1**, 1739 (1970).

<sup>17</sup>A. J. Campillo and C. L. Tang, Appl. Phys. Letters **16**, 242 (1970).

<sup>18</sup>J. Jerphagnon, Appl. Phys. Letters **16**, 298 (1970).

<sup>19</sup>D. H. McMahon, R. A. Soref, and A. R. Franklin, Phys. Rev. Letters **14**, 1060 (1965).

<sup>20</sup>N. Bloembergen and P. S. Pershan, Phys. Rev. **128**, 606 (1962).

<sup>21</sup>G. D. Boyd, A. Ashkin, J. M. Dziedzic, and D. A. Kleinman, Phys. Rev. **137**, A1305 (1965).

<sup>22</sup>R. Bechmann and S. K. Kurtz, in *Crystal and Solid State Physics*, edited by K. H. Hellwege (Springer-Verlag, Berlin, 1969), Vol. 2, p. 176.

<sup>23</sup>J. Jerphagnon (private communication).

<sup>24</sup>M. R. Topp and P. M. Rentzepis, Phys. Rev. A **3**, 358 (1971).

<sup>25</sup>M. Born and E. Wolf, *Principles of Optics* (Pergamon, New York, 1965).

<sup>26</sup>I. B. Berlman, *Handbook of Fluorescence Spectra of Aromatic Molecules* (Academic, New York, 1965).

<sup>27</sup>W. L. Peticolas, R. Morris, and K. E. Rieckhoff, J. Chem. Phys. **42**, 4164 (1965).

<sup>28</sup>A. P. Aleksandrov, V. N. Genkin, G. F. Efremova and A. M. Leonov, Izv. Vysshikh Uchebn. Zavedenii, Radiofiz. **10**, 145 (1967).

<sup>29</sup>I. Webman and J. Jortner, J. Chem. Phys. **50**, 2706 (1969).